

Structural, mechanical, and vibrational properties of $\text{Ga}_{1-x}\text{In}_x\text{As}$ alloys: A molecular dynamics study

Paulo S. Branicio,^{a),b)} Rajiv K. Kalia, Aiichiro Nakano, Jose P. Rino,^{a)} Fuyuki Shimojo,^{c)} and Priya Vashishta

Collaboratory for Advanced Computing and Simulations, Department of Physics and Astronomy, Department of Computer Science, Department of Materials Science and Engineering, University of Southern California, Los Angeles, California 90089

(Received 29 July 2002; accepted 9 December 2002)

Structural, mechanical, and vibrational properties of $\text{Ga}_{1-x}\text{In}_x\text{As}$ ($0 \leq x \leq 1$) random solid solutions are investigated with classical and *ab initio* molecular-dynamics simulations. We find that the Ga–As and In–As bond lengths change only slightly as a function of x , despite the large lattice mismatch ($\sim 7\%$) between GaAs and InAs crystals. The nearest cation–cation distance has a broad distribution, whereas the nearest neighbor anion–anion distance distribution has two distinct peaks. The elastic constants exhibit a significant nonlinear dependence on x . The phonon density-of-states exhibits two high-frequency optical modes. These results are in excellent agreement with experiments. © 2003 American Institute of Physics. [DOI: 10.1063/1.1542681]

Semiconductor alloys have received a great deal of attention because of their potential applications in optoelectronic devices. In these materials, the physical properties can be varied continuously with the composition. This permits continuous tuning of the wavelength of a solid-state laser made of a semiconductor alloy.

A particularly interesting pseudobinary alloy is $\text{Ga}_{1-x}\text{In}_x\text{As}$ ($0 \leq x \leq 1$). At low pressures, it has a simple zinc-blende structure, and it follows Vegard's law (the weighted average of the nearest-neighbor atomic distances is $\sqrt{3}a/4$, where a is the lattice parameter of the alloy).¹ The bond lengths in the binary alloys vary significantly from 2.448 Å in GaAs to 2.623 Å in InAs. Extended x-ray fine structure (EXAFS) measurements² indicate that this large lattice mismatch ($\sim 7\%$) is accommodated by local bond distortions while the zinc-blende structure is preserved. Recently, it has been shown in other semiconductor alloys ($\text{A}_{1-x}\text{B}_x\text{C}$) that the cation-anion bond lengths do not change with x , which is in apparent contradiction with the virtual crystal approximation.³ Besides its intricate structure, $\text{Ga}_{1-x}\text{In}_x\text{As}$ also exhibits complex vibrational properties. The nature of optical phonons in $\text{Ga}_{1-x}\text{In}_x\text{As}$ is not well understood. Experimental data indicate either a mixed-mode⁴ or a two-mode⁵ behavior.

In this letter, we report classical and *ab initio* molecular-dynamics (MD) simulation studies of the $\text{Ga}_{1-x}\text{In}_x\text{As}$ ($0 \leq x \leq 1$) alloys. We investigate the structural, mechanical, and dynamical properties for composition ranging from $x = 0$ (GaAs) to $x = 1$ (InAs). We find that the Ga–As and In–As bond lengths change slightly with x despite the large lattice mismatch between GaAs and InAs crystals. The nearest cation–cation distance has a broad distribution, whereas the As–As distribution has two near neighbor peaks. The

phonon density-of-states exhibits two high-frequency optical modes. The elastic constants vary significantly with x .

The interatomic potential used in the classical MD simulations consists of two- and three-body terms.⁷ (Recently, classical MD studies of similar alloys using Tersoff based potentials have been reported.⁶) The two-body terms include steric repulsion, long-range Coulomb interactions resulting from charge transfer, and induced charge-dipole and dipole–dipole interactions due to large electronic polarizability of anions. The three-body interaction consists of covalent bond-bending and bond-stretching terms. The potentials for pure GaAs ($x = 0$) and InAs ($x = 1$) alloys are validated by comparing simulation results with experimental values of the lattice constants, cohesive energies, elastic constants, melting temperatures, structural transition pressures, phonon densities-of-states, and neutron static structure factors for amorphous systems.⁷ For intermediate values of x , an interpolation scheme is used to obtain the dependence of the potential on the local chemical environment.⁸ The interatomic potential between Ga and In is an arithmetic average of the Ga–Ga potential in GaAs and the In–In potential in InAs. We find that simulation results are not sensitive to small variations in this interpolation rule. The interaction between two As atoms is obtained from linear interpolation between As–As potentials, $\nu_{\text{AsAs}}^{(0)}$ and $\nu_{\text{AsAs}}^{(1)}$, in GaAs and InAs, respectively,

$$\nu_{\text{AsAs}}^{(m,n)} = \left(1 - \frac{m+n}{8}\right) \nu_{\text{AsAs}}^{(0)} + \frac{m+n}{8} \nu_{\text{AsAs}}^{(1)},$$

where m and n are the numbers of nearest-neighbor In atoms around the two As atoms. The three-body Ga–As–In potential is taken to be the average of the Ga–As–Ga potential in GaAs and the In–As–In potential in InAs. The rest of the terms in the potential are identical to those in pure GaAs and InAs potentials.

The initial configuration of the MD simulation is prepared by substituting Ga atoms with In randomly with probability x in the zinc-blende GaAs crystal. The system is ther-

^{a)}Also at: Universidade Federal de São Carlos, São Carlos, São Paulo, Brazil.

^{b)}Electronic mail: ppsb@lsu.edu

^{c)}Also at: Kumamoto University, Kumamoto, Japan.

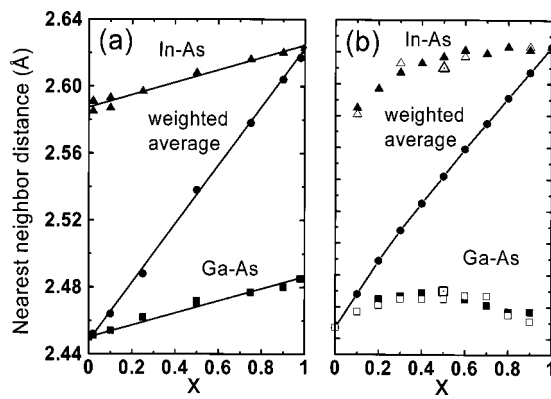


FIG. 1. (a) EXAFS data on Ga-As (squares) and In-As (triangles) nearest-neighbor distances as a function of alloy composition. Also shown is the weighted average (circles) of the bond lengths, which is the virtual-crystal approximation value calculated from the lattice constant measured by x-ray diffraction. (b) The MD results for the same quantities (solid symbols) for a 1000-atom system. Also shown are Ga-As (squares) and In-As (triangles) nearest-neighbor distances for a 216-atom system in MD (open symbols) and *ab initio* MD (dotted open symbols) simulations.

malized at 500 K for 10 000 steps. Subsequently, the steepest descent quench method is used to bring the system to a local minimum-energy configuration. The simulations are performed for systems with 216, 1000, and 8000 atoms. We find that size effects are negligible.

We have also performed *ab initio* MD simulations for a 216-atom system. The calculations⁹ are based on the local density approximation in the framework of density functional theory.^{10,11} We employ a high order finite-difference approximation to the kinetic energy,¹² multigrid acceleration,¹³ and nonconserving pseudopotentials.¹⁴ The calculations are performed on a 128-processor SGI Origin 2000 using spatial decomposition and message passing interface.⁹ Atomic positions are relaxed with MD simulations, where atomic forces are calculated from the Hellmann-Feynman theorem.

From the classical MD simulations we have computed pair distribution functions (PDF) to analyze the cation-anion structural correlations and compare the results with EXAFS experimental data² [Fig. 1(a)]. We find a well-defined split in

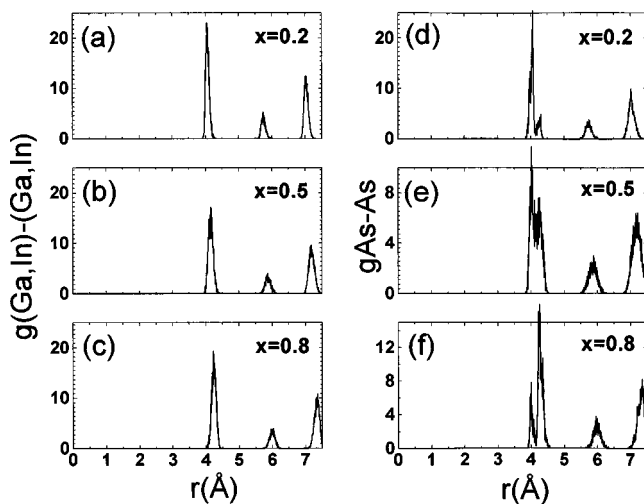


FIG. 2. MD pair distribution functions for cation-cation pairs (a)-(c) and As-As pairs (d)-(f), at temperature 10 K. The nearest cation-cation distance has a broad distribution, whereas the nearest As-As has two distances.

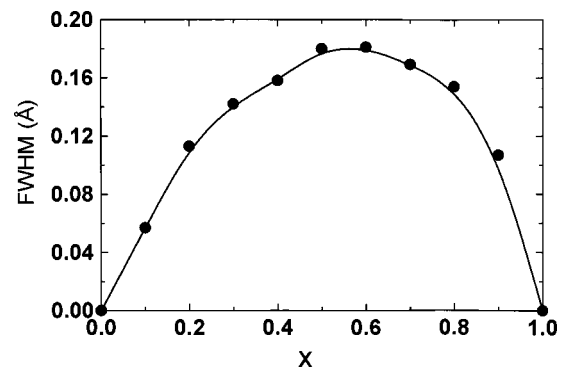


FIG. 3. Full width at half maximum of the first peak of the cation-cation pair distribution function, which quantifies the disorder at the first shell of the cation sublattice in $\text{Ga}_{1-x}\text{In}_x\text{As}$.

the first neighbor shell (two-mode behavior) corresponding to Ga-As and In-As pairs, respectively. The peak position, plotted in Fig. 1(b) for various x values, indicate that the bond lengths of Ga-As and In-As are insensitive to variations in x . This observation is in contradiction with the virtual crystal approximation,³ as well as with Pauling's assumption that the atomic radii are conserved quantities.¹⁵ In Fig. 1(b), MD results for 1000 and 216 atoms demonstrate that the size effect is negligible. We have also included the *ab initio* MD results for $x=0.5$ to show that the main features of the classical MD are robust. Figure 1(b) also shows the weighted average of the bond length. As expected, the weighted bond length follows Vegard's law and is identical to $\sqrt{3}a/4$. These MD results are in good agreement with EXAFS data² and valence force-field calculations.¹⁶

The PDFs, shown in Figs. 2(a)-2(c), represent the cation-cation sublattice structure. The results are in good agreement with the virtual crystal approximation for atoms at a single distance. However, the PDFs shown in Figs. 2(d)-2(f) exhibit a split in the anion-anion distribution, suggesting the existence of two As-As neighbor distances. This is also in good agreement with experiments.²

We also observe broadening of PDF peaks due to disorder in both cation-cation and anion-anion distributions. In order to quantify this disorder, the full-width-at-half-maximum of the first peak in cation-cation PDF is plotted in Fig. 3. Most of the disordered structure is observed at inter-

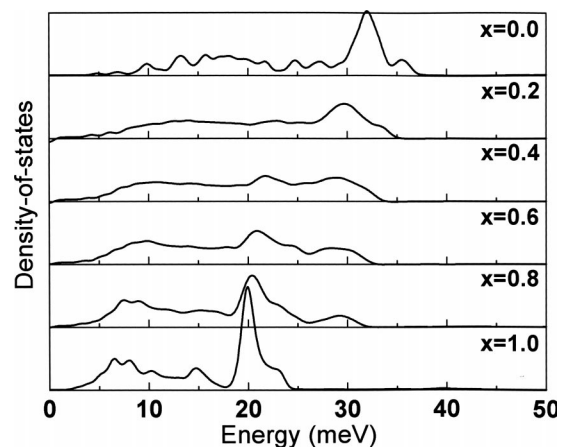


FIG. 4. Phonon density-of-states for $\text{Ga}_{1-x}\text{In}_x\text{As}$ alloys obtained by MD simulations.

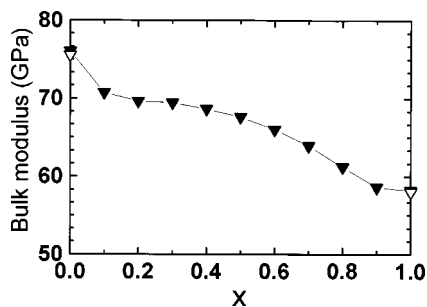


FIG. 5. Bulk modulus obtained by MD simulations (solid symbols) as a function of alloy composition, x . For $x=0$ (GaAs) and $x=1$ (InAs), experimental data are shown with open symbols.

mediate values of x ($0.5 < x < 0.6$). The structure at high In concentrations ($x > 0.5$) is more disordered than at high Ga concentrations ($x < 0.5$). These results are in complete accord with EXAFS data.²

Figure 4 shows the phonon density-of-states calculated from the Fourier transform of the velocity autocorrelation function. For $x=0$ (GaAs) and $x=1$ (InAs), our MD results agree well with experimental data¹⁷ and *ab initio* electronic-structure calculations.¹⁸ For intermediate x values, experimental data on optical phonons at high frequencies are controversial. Theoretically, two types of distributions are found at high frequencies in $A_{1-x}B_xC$ alloys. In one instance, a band of frequency varies continuously from the frequency for the AB to the frequency corresponding to BC, with the strength of the band remaining nearly constant. In the two mode distribution, two bands of frequencies, close to those in binary systems (AB and BC), persist in the mixed crystal, with the strength of each band increasing from zero to a maximum value as the concentration of the corresponding constituent increases. In an earlier study,⁴ the optical modes of the $Ga_{1-x}In_xAs$ alloys were found to have a mixed mode. However, a recent experiment supports the two-mode scenario.⁵ Figure 4 unambiguously shows two modes in the $Ga_{1-x}In_xAs$ alloys. For intermediate values of x ($0.2 < x < 0.8$), significant broadening of the peaks is observed. This may arise from substitutional disorder-assisted mixing of phonon modes due to lattice distortion.

Figure 5 shows our results for the bulk modulus of $Ga_{1-x}In_xAs$. The bulk modulus has a considerable nonlinear dependence on the composition. For $x=0$ (GaAs) and $x=1$ (InAs), our results are in good agreement with experimental data, which are also shown in Fig. 5.

In summary, MD simulations of the pseudobinary alloys, $Ga_{1-x}In_xAs$, reveal that the local distortion in the crystal lattice gives rise to two well-defined bond lengths, Ga–As and In–As. The cation sublattice exhibits broad distribution around first-neighbor shell, whereas the As sublattice has two As–As neighbor distances. The phonon density-of-states has two high-frequency modes typical of optical modes in binary materials. These results are in excellent agreement with experimental results, and also with our *ab initio* MD simulation results. The calculated bulk modulus of the alloy varies significantly with the composition x .

This work was supported by NSF, DOE, AFOSR, ARL, USC-Berkeley-Princeton-LSU-DURINT, and NASA. Simulations were performed on parallel computers in the Concurrent Computing Laboratory for Materials Simulations at Louisiana State University and DoD's Major Shared Resource Centers under a DoD Challenge project. One of the authors (P.S.B.) would like to acknowledge the Brazilian fellowship (FAPESP) for support.

¹L. Vegard, Z. Phys. **5**, 17 (1921).

²J. C. Mikkelsen and J. B. Boyce, Phys. Rev. Lett. **49**, 1412 (1982); Phys. Rev. B **28**, 7130 (1983); J. Cryst. Growth **98**, 37 (1989).

³See, for example, J. C. Phillips, *Bonds and Bands in Semiconductors* (Academic, New York, 1973), p. 214.

⁴M. H. Brodsky and G. Lucovsky, Phys. Rev. Lett. **21**, 990 (1968).

⁵J. Groenen, R. Carles, G. Landa, C. Guerret-Piécourt, C. Fontaine, and M. Gendry, Phys. Rev. B **58**, 10452 (1998).

⁶M. A. Migliorato, A. G. Cullis, M. Fearn, and J. H. Jefferson, Phys. Rev. B **65**, 115316 (2002).

⁷I. Ebbsjö, R. K. Kalia, A. Nakano, J. P. Rino, and P. Vashishta, J. Appl. Phys. **87**, 7708 (2000).

⁸D. W. Brenner, Phys. Status Solidi B **217**, 23 (2000); M. Z. Bazant, E. Kaxiras, and J. F. Justo, Phys. Rev. B **56**, 8542 (1997).

⁹F. Shimojo, R. K. Kalia, A. Nakano, and P. Vashishta, Comput. Phys. Commun. **140**, 303 (2001).

¹⁰P. Hohenberg and W. Kohn, Phys. Rev. **136**, B864 (1964).

¹¹M. L. Cohen, Science **261**, 307 (1993).

¹²J. R. Chelikowsky, N. Troullier, K. Wu, and Y. Saad, Phys. Rev. B **50**, 11355 (1994).

¹³E. L. Briggs, D. J. Sullivan, and J. Bernholc, Phys. Rev. B **54**, 14362 (1996).

¹⁴N. Troullier and J. L. Martins, Phys. Rev. B **43**, 8861 (1991).

¹⁵L. Pauling, *The Nature of the Chemical Bond* (Cornell University Press, Ithaca, NY, 1967).

¹⁶J. L. Martins and A. Zunger, Phys. Rev. B **30**, 6217 (1984).

¹⁷C. Patel, W. F. Sherman, G. E. Slark, and G. R. Wilkinson, J. Mol. Struct. **115**, 149 (1984).

¹⁸P. Giannozzi, S. de Gironcoli, P. Pavone, and S. Baroni, Phys. Rev. B **43**, 7231 (1991).